Metal-Containing Homopolymers Showing a Paramagnetic Nematic Mesophase

Mercedes Marcos, Luis Oriol, and José Luis Serrano*

Departamento Química Orgánica, Instituto de Ciencia de Materiales de Aragón, Facultad de Ciencias, Universidad de Zaragoza, CSIC, 50009 Zaragoza, Spain

Pablo J. Alonso

Departamento Física de la Materia Condensada, Instituto de Ciencia de Materiales de Aragón, Facultad de Ciencias, Universidad de Zaragoza, CSIC, 50009 Zaragoza, Spain

José Antonio Puértolas

Departamento Ciencia de Materiales, Instituto de Ciencia de Materiales de Aragón, ETSII, Universidad de Zaragoza, CSIC, 50015 Zaragoza, Spain

Received February 9, 1990

ABSTRACT: We have synthesized and characterized new homopolyesters containing paramagnetic units. Bis(*N*-R-4-hydroxysalicylaldiminato)copper(II) compounds (R = $-C_nH_{2n+1}$, n = 1, 5, and 10) were condensed with an acid dichloride in order to obtain the target polymers. Mesomorphic melts below the decomposition temperatures were observed except for n = 1. EPR and DSC measurements showed two different crystalline forms. In one of them, Cu^{2+} was in an environment close to a square-planar coordination. An isotropic EPR signal was observed and could be related to Cu–Cu or Cu–O interactions among different metallomesogens in the neighborhood. These compounds gave evidence of some degradation under electric fields.

Introduction

The synthesis of new metal-containing liquid crystals is the subject of increasing interest. Metals enable us to study the effect of new geometries on mesogenic properties.[1,2] Moreover, the choice of the correct metal ion can introduce unusual electrooptic and magnetic properties.[3-6] However, there are still not many references with regard to liquid-crystal polymers containing metallomesogens.[7-10] These materials could be of interest as a means of controlling molecular orientation with respect to the magnetic field by the introduction of paramagnetic units in polymer chains.[11]

We report on the synthesis of new metal-containing liquid-crystal homopolymers (coded [N*n*Cu][P10]) obtained by the condensation of functionalized copper(II) complexes and acid dichlorides.

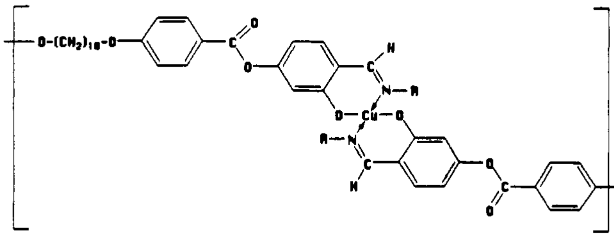

R = $-(C_nH_{2n+1})$, n = 1, 5 and 10

[NnCu][P10]

Electron paramagnetic resonance (EPR) spectra and dielectric measurements were carried out in order to study the possible orientation of polymers.

Interfacial polymerization proved to be the most suitable way of obtaining the polymers. They were characterized by infrared spectroscopy (IR), elemental analysis, viscosimetry, and vapor pressure osmometry (VPO). Their thermal properties were characterized by differential scanning calorimetry (DSC) and thermogravimetric and derivative thermogravimetric analysis (TGA and DTG). Optical microscopy (OM) and miscibility studies were used to characterize the mesogenic compounds.

Experimental Section

Synthesis of Monomers. The synthetic procedure leading to the target polymers is outlined in Scheme I.

Bis(*N*-alkyl-4-hydroxysalicylaldiminato)copper(II) compounds (IV = [N*n*Cu], *n* = 5 and 10) were synthesized by using the Sacconi method:[12] 4 mmol of complex bis(4-hydroxysalicylaldehydato)copper(II)[13] and 8 mmol of the appropriate primary amine were refluxed in 10 mL of ethanol until solution was complete. After cooling in the refrigerator overnight, a precipitate was separated, washed with cool ethanol, and purified by precipitation twice from solutions of acetone.

Bis(*N*-methyl-4-hydroxysalicylaldiminato)copper(II) ([N1Cu]) was obtained by using an excess of a commercial solution of methylamine (40%) in water. The mixture was refluxed for 30 min and cooled, and the precipitate was filtered and washed with water, methanol, and acetone.

Characterization data are collected in Table I.

1,10-Bis[(chloroformyl)phenoxy]decane (V = [P10]) was obtained according to the Griffin method,[14] recrystallized from carbon tetrachloride, and filtered under nitrogen atmosphere.

Synthesis of Polymers. Sodium hydroxide (4–6 mmol) was dissolved in 40 mL of water and 2 mmol of [N*n*Cu], and 400 mg of benzyltriethylammonium chloride was added. If [N*n*Cu] was insoluble, ethanol was added until the solution was complete. A solution of 2 mmol of [P10] in 50 mL of chloroform was added rapidly, and the mixture was stirred for 10 min. The resulting mixture was poured into about 300 mL of methanol. The precipitated polymer was filtered and washed with water, methanol (twice), and finally acetone. The powdery solids obtained were dried under vacuum over P_2O_5.

Characterization data are collected in Table II.

Techniques. EPR spectra were measured with a Varian E-122 spectrometer working in X-band. For measurements above room temperature (RT) the variable-temperature accessory (E-265) from Varian was used. The powdered samples were placed inside a quartz tube, and the temperature was monitored by a copper–constantan thermocouple attached to the tube. The error in temperature was estimated to be about 0.5 °C.

Dielectric measurements were carried out by using a cell, as previously described.[15] The capacitor is formed by two golden

0024-9297/90/2223-5187$02.50/0

Scheme I

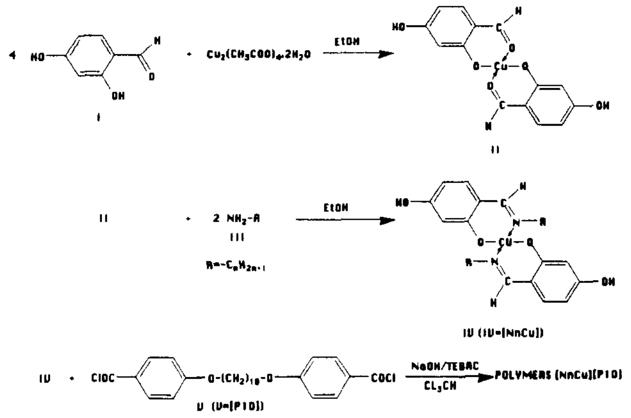

brass circular electrodes of diameter ϕ = 12 mm, with an annular Teflon ring of thickness 500 μm and internal diameter ϕ = 6 mm, as a spacer. The sample was placed inside. The electrical impedance of the capacitor was measured by using a 1689 Precision RLC Digibridge. The temperature of the cell was thermostated to ±0.2 °C, from 20 to 300 °C, by means of a continuous flow of dry nitrogen as a heating element. A platinum resistance thermometer was used to test the temperature of the sample using a Fluke Multimeter. Data acquisition was controlled by a HP-160 microcomputer.

DSC measurements were performed with a Perkin-Elmer DSC-2. The apparatus was calibrated with indium (mp 156.6 °C, heat of fusion 28.4 J/g) and tin (mp 321.9 °C, heat of fusion 60.4 J/g).

TGA and DTG measurements were carried out with a Perkin-Elmer TGS-2 equipped with a System 4 microprocessor controller.

Mesogenic behavior of the polymers was confirmed by optical microscopy using a Meiji polarizing microscope fitted with a Mettler FP-82 heating stage and a FP-80 control unit. Likewise, miscibility studies were performed with a metallonematogen compound: bis[*N*-(4′-ethoxyphenyl)-4-[[(decyloxy)benzoyl]oxy]-salicylaldiminato]copper(II)[16] (C → N 161.3 °C, N → I 254.7 °C).

Inherent viscosity (η_{inh}) was determined by using a Cannon-Fenske viscosimeter at a concentration of 0.5 g/dL in 1,1,2,2-tetrachloroethane at 50 °C.

Number-average molecular weight ($\bar{M}_n$) was determined by using a Knauer vapor pressure osmometer. Measurements were made in 1,1,2,2-tetrachloroethane with benzil as a standard. The operating temperature was 42 °C.

Elemental analyses were carried out with a Perkin-Elmer 240C microanalyzer and IR spectra with a Perkin-Elmer FTIR 1600.

Results and Discussion

Solubility studies showed that [N5Cu][P10] and [N10Cu][P10] are soluble in chlorinated solvents. Stronger solvents might give rise to a progressive depolymerization. 1,1,2,2-Tetrachloroethane was chosen for solution viscosimetry. The results obtained were as follows: [N5Cu][P10], η_{inh} = 0.14 dL/g; [N10Cu][P10], η_{inh} = 0.18 dL/g. [N10Cu][P10] was not entirely soluble, and the result corresponds to the 90% of the sample that was soluble. [N1Cu][P10] proved to be insoluble.

In the case of [N5Cu][P10] $\bar{M}_n$ was measured by VPO. It was found that $\bar{M}_n$ = 4500, which corresponds to a degree of polymerization, n = 5–6, in the oligomeric region.

Thermogravimetric analyses were carried out at 10 °C/min in nitrogen. The polymers showed a 1% weight loss at about 300 °C. The onset of decomposition took place at about 300 °C with two weight losses, one of which can be attributed to the loss of metal-coordinated, alkylamine groups. Both weight losses occurred in the isotropic phase. In addition, isothermic analyses were carried out at 240 °C with [N5Cu][P10]. A weight loss of less than 3% was found after 1 h in nitrogen and air atmosphere.

[N5Cu][P10] and [N10Cu][P10] exhibited mesogenic behavior. Figure 1a shows a polarizing microscopic photograph of [N5Cu][P10] in the mesomorphic state during the second heating cycle. After the first heating cycle a frozen mesomorphic texture could be observed at room temperature when the melt cooled. The nematic mesophase was identified by means of the contact method using a low molecular weight metallonematogen.[16] The high viscosity of the liquid-crystalline melt of the polymer hinders complete diffusion of the reference compound. This may be due either to difficulties in packing macromolecular chains or to the polydispersity of the polymer.[17] When the coverslip was pressed on with a fine steel needle, it was possible to observe a homogeneous nematic phase (Figure 1b).

In the case of [N1Cu][P10] no fusion was observed and the polymer decomposes slowly above 270 °C.

The thermal transitions of the mesogenic polymers were determined by DSC at different heating and cooling rates. Thermal and optical properties are collected in Table III.

Two endothermic peaks corresponding to melting (T_m) and isotropic (T_i) transitions, which agree with optical data, were observed during the first heating. T_m appears as a complex peak with a maximum and a shoulder at low temperatures, which might indicate at least two solution-crystallized forms (Figure 2a).

Annealed samples at temperatures near T_m showed sharper endothermic peaks than untreated samples (Figure 2b).

The second heating showed considerable differences in comparison with the first. A cold recrystallization was observed and the ΔH depended on the cooling rate from the melt. In this way, when a sample of [N5Cu][P10] is quenched from the melt to room temperature, an exothermic transition appears at 100 °C, ΔH = −12.22 J/g, in the second heating. When a sample of the same polymer is cooled at 10 °C/min, this transition appears at 81 °C, ΔH = −4.10 J/g in the second heating. T_m appears at similar temperatures to the first heating. However, a new peak of similar ΔH appears at lower temperatures. Likewise, an important shift of the T_i maximum was observed and could be seen as a shoulder of the T_m peak (Figure 2c). The differences between the first and second heatings could be attributed to two different crystalline forms with a ratio depending on whether the sample was obtained from solution (untreated) or from the melt.

[N5Cu][P10] was chosen in order to carry out EPR and dielectric measurements. The results were interpreted in comparison with a low molecular weight (LMW) analogue (Figure 3).

X-ray diffraction measurements on the nematic phase of the LMW compound were carried out in order to study the orientational order of the sample.[18] This compound showed $\Delta\chi < 0$; therefore, the long molecular axis is aligned perpendicular to the direction of magnetic field. X-ray spectra of the polymer have not been made to date.

EPR Measurements. The EPR spectra of the [N5Cu]-[P10] were measured at different temperatures between room temperature and 245 °C, before and after several heating–cooling cycles. In Figure 4a we show the spectrum taken in a powdered sample at room temperature. From the results obtained after several heating–cooling cycles it can be deduced that this spectrum consists of two signals. One of them, which shows an isotropic character, consists of a broad band centered at $g \approx 2.05$. The other shows two resolved parallel lines, at the low-field part and a barely resolved perpendicular line at the high-field side. Comparing our spectrum with those reported for Cu^{2+} in different polycrystalline and glassy samples,[19,20] we associate this anisotropic signal with Cu^{2+} in a practically

Table I
Yields, Melting Points, Elemental Analysis, and IR Data of Monomers [N*n*Cu]

			elem anal. (calc)				main IR data, cm^{-1}	
monomer	yield, %	mp, °C	C	H	N	Cu[a]	O–H (st)	C=N (st)
[N1Cu]	83	300 (dec)	52.82 (52.20)	4.43 (4.20)	7.70 (7.90)	17.46 (17.70)	3200–2500	1622, 1601
[N5Cu]·H_2O[b]	90	149–151	58.34 (58.91)	6.93 (7.11)	5.67 (5.58)	12.86 (12.85)	3207	1598
[N10Cu]·H_2O[b]	95	110–114	64.37 (64.37)	8.58 (8.86)	4.41 (4.15)	10.02 (9.10)	3205	1599

[a] Determined by TGA of the inorganic residuum at 750 °C in air atmosphere. [b] Hygroscopic compounds.

Table II
Yields, Elemental Analysis, and IR Data of Polymers [N*n*Cu][P10]

			elem anal. (calc)				main IR data, cm^{-1}	
polymer	yield, %	color	C	H	N	Cu[a]	C=O (st)	C=N (st)
[N1Cu][P10]	62	green	64.72 (63.11)	5.70 (6.03)	3.77 (3.25)	8.56 (8.63)	1730	1627
[N5CU][P10]	80	green	67.47 (66.77)	6.84 (7.36)	3.28 (3.12)	7.44 (6.97)	1727	1619
[N10Cu][P10]	76	brown	70.03 (69.34)	7.16 (7.89)	2.06 (2.72)	6.38 (6.87)	1728	1621

[a] Determined by TGA of the inorganic residuum at 750 °C in air atmosphere.

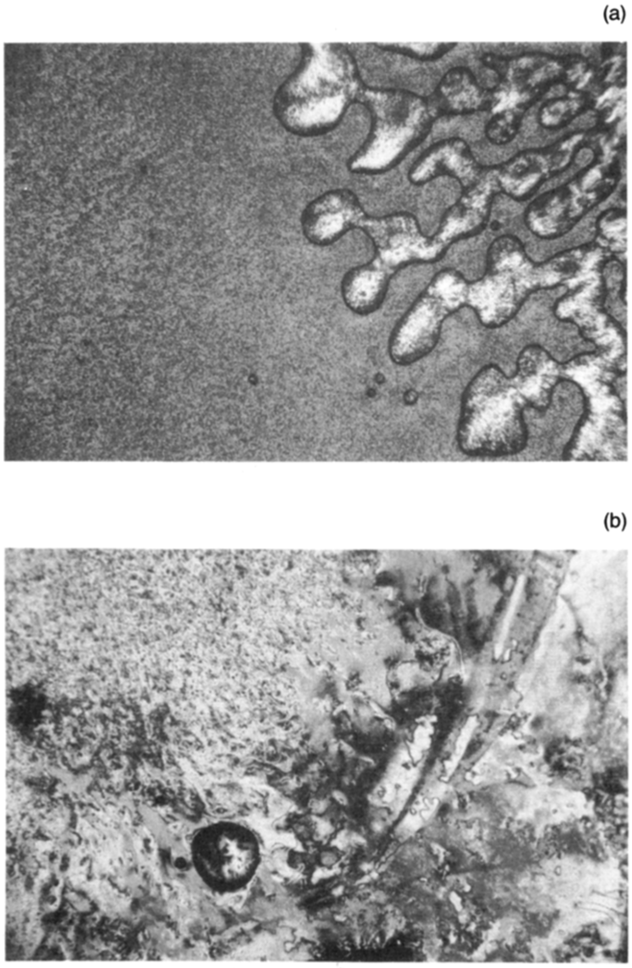

Figure 1. Polarized light micrographs of polymer [N5Cu][P10]: (a) at 220 °C, (b) nematic texture obtained by the addition of bis[*N*-(4′-ethoxyphenyl)-4-[[(decyloxy)benzoyl]oxy]salicylaldiminato]copper(II) taken at 224 °C.

Table III
Thermal and Optical Data of Polymers [N*n*Cu][P10]

	DSC[a]			TGA and DTG data		
polymer	T_m, °C	T_i, °C	OM	1% wt loss	onset	DTG
[N1Cu][P10]	>300 (dec)		dec	302	311	360
[N5Cu][P10]	214	234	nematic	303	299	303
					338	395
[N10Cu][P10]	174	179[b]	nematic	280	263	290
					348	410

[a] Thermal transitions were read during the first heating at the peak maximum positions. Heating rate was 10 °C/min. [b] This transition appears as a shoulder of the T_m peak and depends on the heating rate. The data correspond to a heating rate of 80 °C/min.

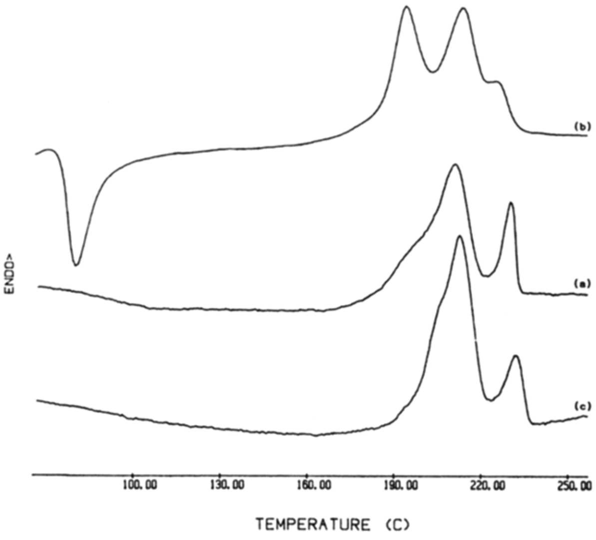

Figure 2. Polymer [N5Cu][P10]: DSC curves, scanning rate 10 °C/min: (a) first heating run, (b) second heating run, (c) first heating run of annealed sample at 186 °C during 1 h.

axial symmetry. The two low-field lines can thus be associated with the outermost lines of the parallel quartet due to the hyperfine splitting while the perpendicular line is not resolved. Copper has two isotopes, ^{63}Cu and ^{65}Cu ($I = {}^3/_2$ for both), with a total 100% natural abundance. Both isotopes have a nearly identical nuclear moment, so the hyperfine splittings are undistinguishable. In this situation and by use of the standard spin Hamiltonian,[21] the following values were obtained for the Hamiltonian parameters: $g_\parallel \approx 2.20$; $g_\perp \approx 2.01$; $A_\parallel \approx 525$ MHz. The values are typical of Cu^{2+} in an environment close to a square-planar configuration having the $|x^2–y^2\rangle$ ground state.

When the sample is heated, the EPR spectrum gradually changes. Figure 4b shows the spectrum taken at 215 °C. At this temperature the solid and nematic phases coexist. It can be observed that the axial Cu^{2+} signal decreases in comparison with the isotropic signal. In fact, if the spectrum is taken at higher temperatures (between 222 and 245 °C), with the sample in either the nematic or isotropic liquid phase, the spectrum consists only of a single isotropic line at about $g \approx 2.08$ (see Figure 4c). This value coincides with that corresponding to the average of the

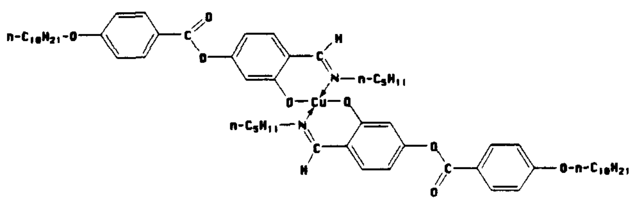

Figure 3. Bis[*N*-*n*-pentyl-4-[[(decyloxy)benzoyl]oxy]salilcylaldiminato]copper(II) used as low molecular weight analogues of [N5Cu][P10].

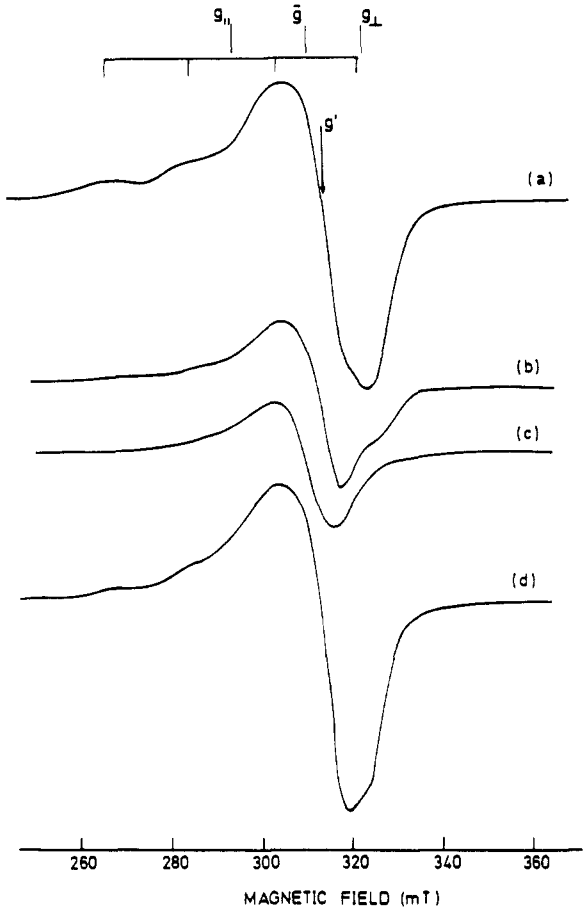

Figure 4. EPR spectra of a sample of [N5Cu][P10]: (a) measured at room temperature, (b) measured at 215 °C (solid and nematic phases coexist), (c) measured at any temperature in the 222–245 °C range (the sample is in the nematic or in the isotropic liquid phase), (d) measured at room temperature after heating at 245 °C and cooling down in presence of a magnetic field of 1.4 T.

g-tensor for Cu^{2+}, $\bar{g} = (g_{\parallel} + 2g_{\perp})/3$. This can be understood if in the high-temperature phases (nematic and isotropic) the metallomesogen groups are able to rotate freely and only a spectrum corresponding to an average spatial orientation is observed.[22]

If the sample is cooled to room temperature, the EPR spectrum is as shown in Figure 4d. At this temperature it is expected that the motion of the metallomesogen groups is frozen. So the features of this spectrum are the same as those of the one given in Figure 4a, but it is noticeable that the relative intensities of the axial Cu^{2+} and the isotropic signal at g' have interchanged. The isotropic signal increases whereas the axial one decreases.

This cooling process was performed either by turning off the magnetic field or under a magnetic field of about 1.4 T, but no significant differences were found in the room-temperature EPR spectrum when it was measured with the dc magnetic field parallel or perpendicular to the direction along which the magnetic field had been directed during the cooling process. This fact could be explained if the anisotropy of the magnetic susceptibility is negative like that of the low molecular weight analogues. Then the long molecular axis can take any orientation perpendicular to the magnetic field.

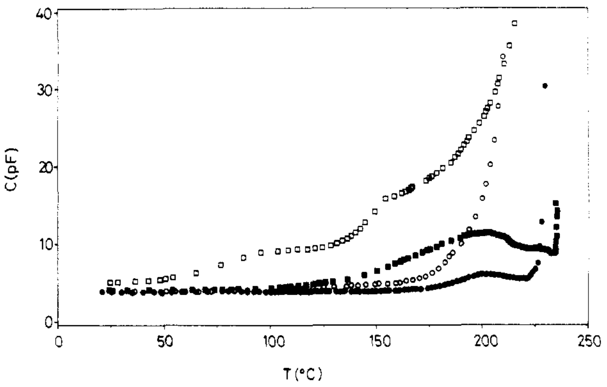

Figure 5. Temperature dependence of the capacitance at 1 kHz: (a,●), (b,■) first heating cycle of the untreated and the annealed sample, respectively, (c,○), (d,□) second heating cycle of the untreated and the annealed sample, respectively.

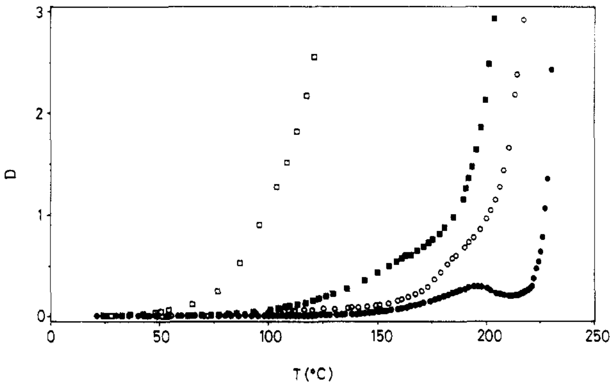

Figure 6. Temperature dependence of the dielectric loss factor at 1 kHz: (a,●), (b,■) first heating cycle of the untreated and the annealed sample, respectively, (c,○), (d,□) second heating cycle of the untreated and the annealed sample, respectively.

Finally we make some brief comments about the isotropic signal. Its g-factor (2.05) is close to that expected for isotropic Cu^{2+}. The appearance of this geometry is difficult to account for, taking into account the structure of the monomer. One explanation for this signal could be the formation of a divalent copper pair,[22] which can in some situations show an isotropic spectrum due to exchange effects.[23] Alternatively, there could be a strong perturbation of the local neighborhood of the paramagnetic entity, giving rise to the formation of different sites for Cu^{2+}, which can be described by a wide distribution of g-factors.[19,24] In this case, oxygen in the neighborhood may serve as the ligand for strong axial interactions.[25]

At present we cannot be sure about the origin of the g'-signal, and further work in order to study this isotropic signal is in progress.

Dielectric Measurements. The temperature dependence of the capacitance, C (pF), and dielectric loss factor (D) of the cell with the sample is shown in Figures 5 and 6, respectively. The measurements were performed at a frequency of 1 kHz and a voltage of 1 V_{rms}. The measurements in Figures 5 and 6 correspond to a heating cycle at a rate of 3–5 °C/min for unaligned specimens.

Figure 5a shows the capacitance results for a sample without previous thermal treatment. The temperature dependence is like a gradual step, with a monotonic increase from 175 to 205 °C and a plateau above that temperature to 222 °C. This last region overlaps the nematic phase of the polymer detected in DSC measurements.

The dielectric loss factor starts to rise at 150 °C and shows a broad shoulder with a maximum at 195 °C (Figure 6a), coinciding with the inflection point of the capacitance measurements.

The above behavior is a typical relaxation process in polymeric liquid crystals.[26] However, due to the structure of our compound we were able to relate the relaxation to an α-process correlated to micro-Brownian motions, similar to other main-chain polymers.[27]

The isotropic–nematic transition was characterized by a quick rise in both magnitudes, above 222 °C, similar to that of a liquid conductor. This conductivity contribution is also observed in combined main-chain side-group liquid-crystal polymers[28] without metallic ions.

After the sample is annealed for 1 h at temperatures below the mesophase, the capacitance results show a similar behavior (Figure 5b). However, two differences were observed. The value of the dielectric constant is higher and the temperature range is wider than in the case of the untreated sample. The behavior of the dielectric loss factor is more significant since, above 162 °C, and superimposed on the shoulder the conducting effect appears at temperatures below the nematic–solid transition (Figure 6b).

When the cooling cycle took place in a magnetic field of 0.3 T, the conducting effect, also present on cooling, masks possible dielectric anisotropy.

The measurements corresponding to the second heating cycle for both kinds of samples are gathered in Figures 5c,d and 6c,d. As can be seen, the conductivity contribution occurs at lower temperatures.

The above behavior could be caused by degradation of these polymers, related to the Cu^{2+} ions. Since the thermogravimetric measurements do not indicate any change in the stability of the compound and the EPR results failed to reveal any modification in Cu^{2+} coordination, we believe that the conducting phenomenon is related to the electric field in the capacitor. New measurements are being carried out in order to determine the influence of the excitation voltage and frequency on the stability of the polymer under an electric field and to study the relaxational process in this main-chain polymer.

Conclusion

The choice of suitable metallomesogens allows mesomorphic melts below the decomposition temperature of metal-containing homopolymers. Bis(*N*-R-4-hydroxysalicylaldiminato)copper(II) monomers disrupt the linearity of rigid cores and introduce flexible *n*-alkylalmine groups, which decrease melting temperatures. This way of reducing the high melting points of main-chain metallomesogen polymers could be compared with the introduction of ring-substituted, crankshaft monomers.[29] We found these monomer complexes more satisfactory than *N*,*N'*-bis(5-hydroxysalicylidenato)(ethylenediamine)copper(II) in order to prove the capacity of transition-metal complexes to induce liquid-crystalline behavior in a homopolymer.[11,25]

The DSC and EPR measurements have similar features. In both, two different crystalline forms could be observed. One of them could be assigned to Cu^{2+} in an environment close to a square-planar configuration without interactions with neighbor molecules.

It is difficult to account for the isotropic signal in the EPR spectrum. This signal could be related to another crystalline form with interactions Cu–Cu or Cu–O among different metallomesogens in the neighborhood. The ratio between the two crystalline forms depends on the previous treatment of the sample. Samples cooled from the melt showed an increase of the isotropic EPR signal, which was connected with the new endothermic peak in the DSC studies.

These polymers showed poor stability under electric fields, which hinders dielectric measurements. However, magnetic fields could be employed in order to control the molecular alignment as it is followed from the previous X-ray diffraction studies of the LMW analogues.

Acknowledgment. The financial support from the EEC (Project No. ST2J-0387-C) and Ministerio de Educacion y Ciencia for a grant to one of the authors is deeply appreciated.

References and Notes

(1) Adams, H.; Bailey, N. A.; Bruce, D. W.; Dhillon, R.; Dunmur, D. A.; Hunt, S. E.; Lalinde, E.; Maggs, A. A.; Orr, R.; Styring, P.; Wragg, M. S.; Maitlis, P. M. *Polyhedron* **1988**, *7*, 1861.

(2) Barberá, J.; Espinet, P.; Lalinde, E.; Marcos, M.; Serrano, J. L. *Liq. Cryst.* **1987**, *2*, 833.

(3) Piechocki, Ch.; Simon, J.; Skoulios, A.; Guillon, D.; Weber, P. *J. Am. Chem. Soc.* **1982**, *104*, 5245.

(4) Chandrasekhar, S.; Sadashiva, B. K.; Srikanta, B. S. *Mol. Cryst. Liq. Cryst.* **1987**, *2*, 833.

(5) Belarbi, A.; Maitrot, M.; Ohta, K.; Simon, J.; André, J. J.; Petit, P. *Chem. Phys. Lett.* **1988**, *143*, 400.

(6) Espinet, P.; Etxebarria, J.; Marcos, M.; Pérez, J.; Remón, A.; Serrano, J. L. *Angew. Chem., Int. Ed. Engl.* **1989**, *28*, 1065.

(7) Takahashi, S.: Morimoto, H.; Takai, Y.; Sonogashira, K.; Hagihara, N. *Mol. Cryst. Liq. Cryst.* **1981**, *72*, 101.

(8) Takahashi, S.; Takai, Y.; Morimoto, H.; Sonogashira, K. *J. Chem. Soc., Chem. Commun.* **1984**, 3.

(9) Carfagna, C.; Caruso, U.; Roviello, A.; Sirigu, A. *Makromol. Chem., Rapid Commun.* **1987**, *8*, 345.

(10) Hanabusa, K.; Higashi, J.; Koyama, T.; Shirai, H. *Makromol. Chem.* **1989**, *190*, 1.

(11) Moore, J. S.; Stupp, S. I. *Polym. Bull.* **1988**, *19*, 251.

(12) Sacconi, L.; Ciampolini, M.; Maggio, F.; Del Re, G. *J. Am. Chem. Soc.* **1960**, *82*, 815.

(13) Pfeiffer, P.; Breith, E.; Lubbe, E.; Tsumaki, T. *Justus Liebigs Ann. Chem.* **1933**, *503*, 84.

(14) Griffin, A. C.; Havens, S. J. *J. Polym. Sci., Polym. Phys. Ed.* **1981**, *19*, 951.

(15) Pérez Jubindo, M. A.; Ezcurra, A.; Etxebarria, J.; Remón, A.; Tello, M. J.; Marcos, M.; Serrano, J. L. *Mol. Cryst. Liq. Cryst.* **1988**, *159*, 137.

(16) Marcos, M.; Romero, P.; Serrano, J. L. *Chem. Mater.* **1990**, *2*, 495.

(17) Noel, C. In *Polymeric Liquid Crystals*; Blumstein, A., Ed.; Plenum Press: New York and London, 1985; p 21.

(18) Presented at the 4emes Journées Francaises des Cristaux Liquides, Montpellier, France, Sept 1989.

(19) Griscon, D. L. *J. Non-Cryst. Solids* **1980**, *40*, 211.

(20) Sands, R. H. *Phys. Rev.* **1955**, *99*, 1222.

(21) Abragam, A.; Bleaney, B. In *Electron Paramagnetic Resonance of Transitions Ions*; Clarendon Press: Oxford, 1970; p 455.

(22) Wertz, J. E.; Bolton, J. R. In *Electron Spin Resonance: Elementary Theory and Applications*; McGraw-Hill: New York, 1972.

(23) See ref 21, p 506.

(24) Marquat, C. L. *Appl. Phys. Lett.* **1976**, *28*, 209.

(25) Shaffer, T. D.; Sheth, K. A. *Mol. Cryst. Liq. Cryst.* **1989**, *172*, 27.

(26) Bormuth, F. J.; Haase, W. *Mol. Cryst. Liq. Cryst.* **1987**, *153*, 207.

(27) Araki, K.; Aoshima, M.; Namiki, N.; Ujiie, S.; Koide, N.; Iimura, K.; Imamura, Y.; Williams, G. *Makromol. Chem., Rapid Commun.* **1989**, *10*, 265.

(28) Kremer, F.; Vallerien, S. U.; Zentel, R.; Kapitza, H. *Macromolecules* **1989**, *22*, 4040.

(29) Chung, T. S. *Polym. Eng. Sci.* **1986**, *26*, 901.